  Bull. Chem. Soc. Jpn., 63, 2487—2493 (1990)

Spin Trapping as Applied to Radicals Produced by the Thermal Decomposition of Di-*t*-butyl Diperoxyoxalate (DBPO) in Aromatic Hydrocarbons

Yoshimi SUEISHI,* Seiji FURUI, Yukinobu MATSUMOTO,
Shunzo YAMAMOTO, and Norio NISHIMURA
Department of Chemistry, Faculty of Science, Okayama University,
Tsushima Naka 3-1-1, Okayama 700
(Received March 1, 1990)

Di-*t*-butyl diperoxyoxalate (DBPO) was allowed to decompose at 40 °C in benzene and xylenes, and transient radicals were trapped by some nitroso compounds. By means of an ESR simulation technique, the trapped radicals were assigned. In benzene, *t*-butoxyl radicals were trapped. Exceptionally, when 1,3,5-tri-*t*-butyl-2-nitrosobenzene(**1**) was used, methoxyl radicals were trapped first, but the ESR signals changed with time and methyl radicals were finally trapped. In xylenes, monomethylbenzyl radicals were exclusively trapped by **1** and 2,4,6-trimethyl-1-nitrosobenzene(**2**). The hyperfine coupling constant (hfcc) of β-hydrogens exhibited a negative temperature dependence for adducts formed between **1** and benzyl radicals(**1-BZ**), while for adducts formed between **2** and benzyl radicals(**2-BZ**), a positive one.

Spin trapping is a convenient technique for the detection and identification of unstable radicals. As traps, nitrones and nitroso compounds are most widely used. In a previous paper,[1] we reported that *N*-*t*-butyl-α-phenylnitrone traps radicals which are produced in the photochemical and thermal decompositions of azoalkanes. However, it has been shown[2,3] that nitroso compounds such as **1** have advantages over nitrones. First, **1** has two trapping sites, the nitrogen and oxygen atoms of the nitroso group, and therefore the trapping will occur either on the nitrogen atom or oxygen atom to produce anilino or nitroxide radicals according to the nature and bulkiness of radicals to be trapped. Secondly, adducts of nitroso compounds afford much more information than those of nitrones in the ESR spectroscopy. Further, adducts of nitroso compounds are usually very stable, and this is the third merit for ESR study.

Terabe and co-workers[3] used 1,2,4,5-tetramethyl-3-nitrosobenzene (**3**) and other nitrosobenzene derivatives and various kinds of radicals produced photochemically and thermally were successfully identified by means of trapping method combined with ESR spectroscopy.

There is extensive work by Bartlett and co-workers[4] on the decomposition mechanism of peresters. Of the peresters, DBPO attracted our interest, since it undergoes a clean decomposition near room temperatures in benzene. According to them, a pair of *t*-butoxyl radicals are separated by two carbon dioxide molecules. This favors for the paired radicals to diffuse apart to each other, avoiding cage reactions. They discussed the reaction scheme on the basis of product analysis.

In the present research, radical species produced by the thermal decomposition of DBPO in some aromatic hydrocarbons were trapped by a series of nitroso compounds, and trapped radicals were identified. From the kinds of trapped radicals and their stabilities, a plausible reaction scheme has been proposed.

The temperature dependence of the hfcc's of the spin adducts can provide information about the conformations and barriers to hindered internal rotation.[5-7] Studies so far have concerned simple radicals of comparatively low rotational barriers (~10 kJ mol^{-1}). In this work, the temperature dependence of the hfcc of β-hydrogen was examined for crowded spin adducts produced in xylenes, and briefly discussed in relation to the conformation of the adducts.

Experimental

Materials. Following nitroso compounds were used.

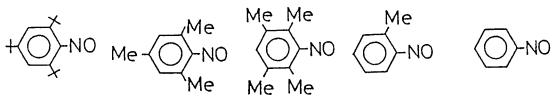

1 **2** **3** **4** **5**

Compounds **1** and **5** were purchased from Aldrich Chemical Company, Inc., and were used without further purification.

Compound **2** was prepared as follows.[8] Peroxybenzoic acid was prepared by the method of Ogata and Sawaki.[9] The acid (30 ml) was added with stirring to a 100 ml chloroform solution containing 10 g of 2,4,6-trimethylaniline. After reaction, **2** was isolated and washed with 2% sodium thiosulfate solution and then with 5% sodium carbonate solution. By recrystallization from absolute methanol, white, plate-like crystals were obtained; mp 120—121 °C (lit,[8] 122 °C).

Compound **3** was prepared from durene as a starting material, according to the method of Smith and Taylor; mp 160 °C, decomp (lit,[10] 160 °C).

Compound **4** was obtained by oxidizing 2-methylaniline with peroxybenzoic acid in dichloromethane and purified by chromatography on alumina and by recrystallization.[11] Yellow crystals; mp 48 °C, decomp.

DBPO was prepared from *t*-butyl hydroperoxide which was prepared as follows.[12] To a mixture of *t*-BuOH (1 mole) and 70% H_2SO_4 (1 mole) was added at 0—5 °C with stirring a 27% H_2O_2 (1 mol) solution. The mixture separated into aqueous and organic layers. The organic layer was neutralized with a $MgCO_3$ suspension, washed with water, and dried over anhydrous $MgSO_4$. The *t*-Butyl hydroperoxide was distilled under a reduced pressure (20 mm Hg). DBPO was prepared as follows.[4] A solution of oxalyl dichloride (3.2 g) in 25 ml anhydrous hexane was added dropwise to a cold solution of *t*-butyl hydroperoxide (4.5 g) and pyridine (4 g) in 50 ml of hexane, the temperature of the solution being kept below 0 °C. After reaction, pyridinium chloride crystals were removed. The filtrate was cooled in a Dry Ice–acetone mixture and allowed to stand to precipitate DBPO. The peroxy ester was recrystallized from a small amount of hexane, and stored at −25 °C in a freezer; mp 52 °C, decomp (lit,[4] 50.5—51.5 °C). Using $(CD_3)_3COH$ as a starting material, DBPO-d_{18} was synthesized in the same manner as described above; mp 52 °C, decomp.

Solvents were of guaranteed grade and were used after purification in the usual manner.

ESR Measurements. A JEOL JES-FE3XG spectrometer equipped with a 100-kHz field modulator and a TE 011 cavity was used for ESR measurements. A sample solution containing ca. 10^{-3} mol dm^{-3} DBPO and ca. 10^{-2} mol dm^{-3} nitroso compound was deaerated by bubbling nitrogen gas. The solution was transferred into a quartz tube and the tube was set in the cavity after flushing again with nitrogen. In some cases, dissolved oxygen was removed by the freeze-and-thaw method. DBPO was allowed to decompose at 40 °C, and ESR spectra of spin adducts of transient radicals produced were recorded on the spectrometer. The temperature in the cavity was controlled by a JEOL variable temperature regulator. Spectral simulations were made with an attached computer. The *g*-values of the spin adducts relative to that of Fremy's salt (g=2.0055) or 2,2-diphenyl-1-picrylhydrazyl (g=2.0036) were estimated in the usual manner.

Results and Discussion

Thermal Decomposition of DBPO and DBPO-d_{18} in Benzene in the Presence of 1. DBPO was allowed to decompose at 40 °C in benzene in the presence of **1**. Within a few minutes, ESR signals as shown in Fig. 1a appeared first, but the intensity of the signals gradually decreased and new signals appeared at the expense of the first signals. Figure 2a is the newly appeared signals taken about 30 min after the decomposition had started. In view of the decomposition mechanism of DBPO,[4] we considered at first that the following spin adduct must be responsible for the first signals.

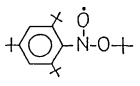

A-1

It is notable that the hfcc due to the nitroxide nitrogen is a_N=23.80 G, remarkably larger than the usually observed one (10—15 G)(1G=10^{-4} T). A comment for this will be made later.

The hyperfine structure (hfs) is embarrassing and its assignment has been unsuccessful for a long time. In the light of literature,[3] the meta hydrogens may be involved, but this alone cannot explain the hfs in Fig. 1a. As a result of trial-and-error, we noticed that if three "equivalent" hydrogen atoms are assumed to participate in the hfs, the ESR spectrum can be reproduced well by means of the simulation technique. Fig. 1b is the simulated spectrum with

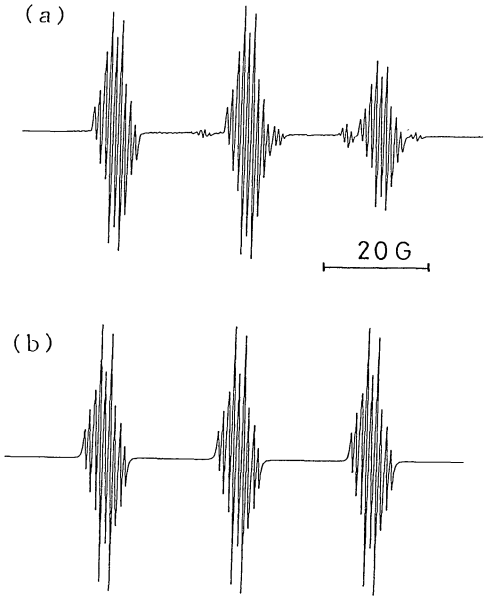

Fig. 1. (a) Experimental and (b) simulated ESR spectra of **A-2**.

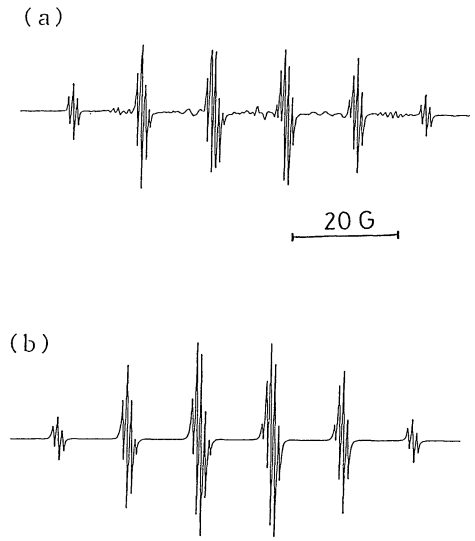

Fig. 2. (a) Experimental and (b) simulated ESR spectra of **A-3**.

a_N=23.80 G, a_{m-H}=0.81 G, and a_{3H}=1.86 G. Methyl protons in the *t*-BuO group are a possible and conceibable source. However, the steric circumstance around the nitroso group is extremely severe, and free rotation of any methyl groups in the *t*-BuO group is unlikely. Moreover, the 3H hfcc-value is too large to be attributed to the methyl hydrogens. Thus the assumed adduct **A-1** cannot be responsible for the first signals.

By chance, we noticed that the reported hfcc-values for the adduct **A-2**[13] which was formed from γ-irradiated methanol in the presence of **1**, agreed well with ours. Therefore, it is almost unequivocal that the signals in Fig. 1a correspond to **A-2.** The spectrum in Fig. 2a can be assigned to the following spin adduct **A-3** with a_N=13.03 G, a_{m-H}=0.81 G, and $a_{\beta-H}$=12.33 G.

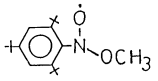

A-2

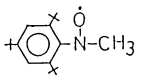

A-3

The simulated spectrum is shown in Fig. 2b. It is noted that the a_N-value is normal one. The problem is how the adduct **A-2** was formed from the *t*-BuO· radical.

Bartlett and co-workers[4] studied the thermal decomposition of DBPO in benzene. In accordance with their results, it is unlikely that methoxyl radicals are formed from the direct decomposition of *t*-butoxyl radicals. Therefore, we tentatively assume a following transient species through which the methoxyl group is trapped. Allowing for the time lag for the appearances of the spin adduct **A-3**, a plausible reaction scheme in this system would be as follows:

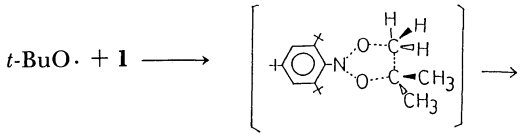

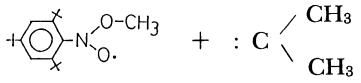

A-2

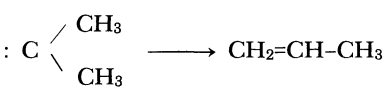

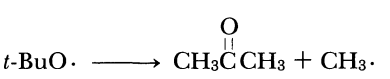

$$CH_3\cdot + \mathbf{1} \longrightarrow \mathbf{A\text{-}3}$$

$$CH_3\cdot + \mathbf{A\text{-}2} \longrightarrow \mathbf{A\text{-}3} + CH_3O\cdot$$

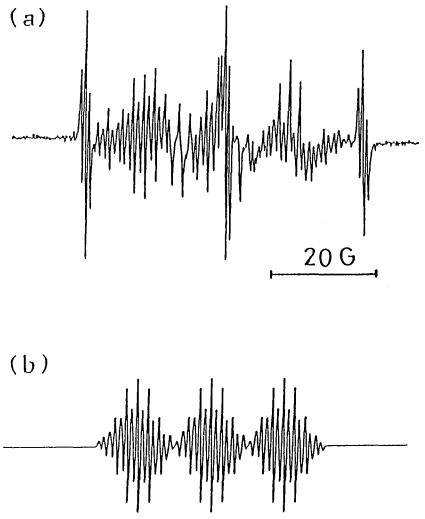

Fig. 3. (a) ESR signals obtained during the thermal decomposition of DBPO-d_{18} in the presence of **1** in benzene-d_6. (b) Simulation spectrum for **A-5**.

The fate of the $CH_3O\cdot$ radicals freed from **A-2** is not obvious; they will presumably be trapped by **1** or react with methyl radicals to form dimethyl ether. The above scheme is partially in harmony with the results of Bartlett et al.

In this respect, we considered that deuterium substitution will afford a useful information. Along this line, DBPO-d_{18} was prepared and allowed to decompose in benzene-d_6 in the presence of **1**. The ESR signals obtained are shown in Fig. 3a. We can see a well-defined triplet (1:1:1) of triplet (1:2:1) spectrum which can be assigned to **A-4**. A drastic change in the spectral pattern clearly indicates that the three protons in question have come from the *t*-BuO group.

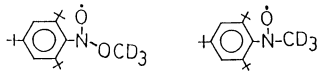

A-4

A-5

Although they are not well-characterized, the species **A-5** will be responsible for the remaining signals in Fig. 3a. The simulated spectrum with a_N=12.97 G, a_{m-H}=0.81 G, and $a_{\beta-D}$=1.95 G for **A-5** is shown in Fig. 3b. It is noted that the ratio $a_{\beta-H}/a_{\beta-D}$=6.3 is very close to the ratio (=6.5) of the Fermi hfcc's for H and D. Similar H-hfcc (13.2 G) and D-hfcc (2.0 G) are reported for *t*-BuN(Ȯ)CH_3 and *t*-BuN(Ȯ)CD_3, respectively.[14]

Spin Trapping by Use of 2, 3, 4, and 5 in Benzene. In place of **1**, traps **2**, **3**, **4**, and **5** were used and transient radicals were trapped. In contrast to **1** the following spin adducts were formed.

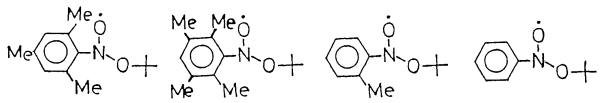

A-6 **A-7** **A-8** **A-9**

ESR spectra for **A-6** (a_N=24.45 G) and **A-8** (a_N=16.10 G) are shown in Figs. 4a and 5a together with their simulated ones. Judging from these ESR signal patterns, the possibility that methoxyl radicals were trapped could be eliminated. When **3** was used, a (poorly resolved) doublet of triplet spectrum with a_N=25.00 G (lit,[3] 25.18 G) appeared. In spite of structural similarity around the N–O group between **2** and **3**, the hfs tentatively assigned to the ortho methyl hydrogens for **A-6** did not appear for **A-7**. The signals of **A-6** and **A-8** survived longer than half a day. This is a remarkably different point from **A-2**. In the light of such large N hfcc it is almost certain that alkoxyl radicals were trapped by **2** and **3**. In case of the traps **2—4**, steric circumstances around the nitroso group are less severe than those of **1** and therefore, trapped radicals must be *t*-BuO·.

The hfcc's and *g*-values for the various kinds of adducts are given in Table 1. By inspection of the data in Table 1, we notice that the a_N-values for the *t*-BuO-adducts decrease in the order:

o,o'-Disubstituted>*o*-Monosubstituted>Unsubstituted

This order agrees with the order of decreasing steric hindrance around the =N–O group. Discussion for this will be made later. In nitroxide radicals, the electron spin on the nitroxyl oxygen atom flows onto the neighboring N atom through resonance hybrid as indicated below.

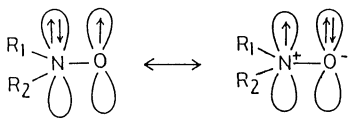

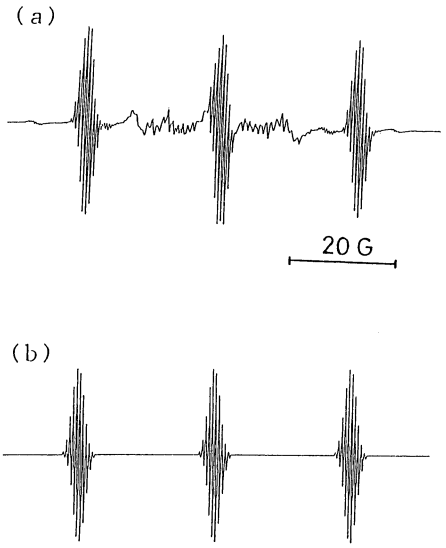

Fig. 4. (a) ESR signals of the adduct of **2** with *t*-BuO, and (b) its simulation spectrum.

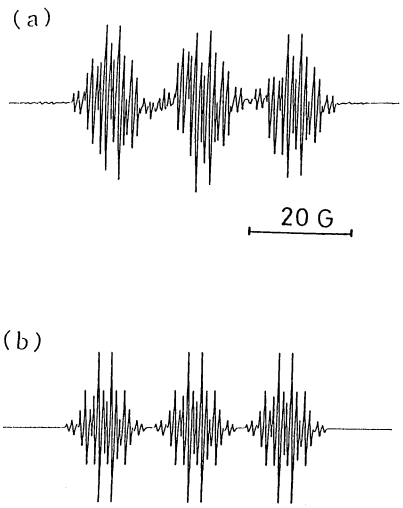

Fig. 5. (a) ESR spectrum assigned to **A-8**, and (b) simulation spectrum.

Table 1. ESR Parameters for Some Nitroso Spin Adducts (Reported Values in Parentheses)

			Ar–N–R O		hfcc/G		
Ar–N=O	R	Solvent	g-Value	a_N	$a_{m\text{-H}}$	$a_{\beta\text{-H}}$	Other
1	OCH_3	Benzene	2.0063	23.80	0.81		1.86[a]
		CH_3OH	(2.0063	24.0	0.9		2.0)[13]
1	CH_3	Benzene	2.0066	13.03	0.81	12.33	
1	OCD_3	Benzene-d_6		24.80	0.76		
1	CD_3	Benzene		12.97	0.81	1.95	
2	*t*-BuO	Benzene	2.0059	24.45	0.74		0.55[b]
3	*t*-BuO	Benzene	2.0054	25.00			0.20[c]
		Benzene	(2.0054	25.18)[3]			
4	*t*-BuO	Benzene	2.0052	16.10	0.92		2.36[d] 0.92[e]
5	*t*-BuO	Benzene	2.0068	14.20	1.09		2.90[f]
		$CFCl_3$		(14.9	1.0)[15]		

a) a_{CH_3O}, b) $a_{o\text{-}CH_3}=a_{p\text{-}CH_3}$. c) $a_{p\text{-H}}$ (poorly resolved doublet). d) $a_{o,p\text{-H}}$. e) $a_{o\text{-}CH_3}$ (tentatively assigned). f) $a_{o\text{-H}}=a_{p\text{-H}}$.

According to the view of Ingold and co-workers,[16–18] the right-hand side structure is destabilized if R_1, R_2 are electron-withdrawing groups resulting in the reduced a_N-value. Of hundreds of nitroxide ESR data, summarized in Landolt Börnstein, New Series,[19] the a_N-values are between 10 and 15 G for most nitroxides. There is an exceptional group of nitroxides i.e., alkoxy alkyl nitroxides; their N hfcc-values are between 24 and 29 G. Chatgilialoglu and Ingold[18] considered without explicit proof that the enhanced N hfcc's are a consequence of increased nonplanarity at N, since a nonplanar structure permits to increase in the s character of the semioccupied orbital on N. When 2,6-disubstituted aryls (**2, 3**) are used, the N hfcc-values are comparable to those of alkyls. In these adducts, the steric hindrance will be severe and the phenyl ring will take a position perpendicular to the $-N(\dot{O})R_1$ quasi-plane, and flow of spin into the benzene ring will be forbidden. The steric hindrance will become much less severe for **A-9**, and spin can flow into the phenyl group resulting in the reduced a_N-value. A very small value of a_{p-H} for **A-7** compared with those for **A-8** and **A-9** supports the above view. Judging from the *g*-values in Table 1, all the adducts can safely be regarded as nitroxide radicals instead of anilino radicals.

Thermal Decomposition of DBPO in the Presence of 1 or 2 in Xylenes. In place of benzene, *o*-, *m*-, and *p*-xylenes were used as solvent. The ESR spectra obtained during the thermal decomposition of DBPO in the presence of **1** are shown in Fig. 6. It is obvious that monomethylbenzyl radicals are exclusively trapped by **1**. This can be justified by the fact that the methyl hydrogens are much more easily abstracted by *t*-BuO· radicals than the benzene hydrogens.[20] It follows that the *t*-BuO· radical abstracts one of the xylene methyl hydrogens. The estimated hfcc's for N, β-H and *m*-H are given in Table 2. When **2** was used, a different pattern of ESR signals appeared. A representative one is shown in Fig. 7. Overlappings of very small hfcc's due to *m*-H and *o,p*-methyl hydrogens of the trap side may be responsible for the line broadening. In fact, the hfcc-values for *m*-H, *p*-H, and o-methyl hydrogens in 2,6-dimethyl-substituted nitrosobenzenes are considerably smaller than those of the corresponding unsubstituted or monosubstituted nitrosobenzene (Table 1). We notice two distinctions in the hfcc: first, the $a_{\beta-H}$ values for the **1-BZ** adducts are larger than those for the **2-BZ** adducts and secondly, the hfcc due to the *m*-H is not observed for the latter adducts. It is notable that the a_N values in Table 2 are larger than those for N-alkyl phenylnitroxide (ca. 10 G),[21] due to enhanced steric hindrance.

Table 2. ESR Parameters for Spin Adducts Formed in Xylenes at 40°C

Trap	Solvent	*g*-Value	a_N/G	$a_{\beta\text{-H}}$/G	$a_{m\text{-H}}$/G
1	*p*-Xylene	2.0060	13.91	14.55	0.82
	m-Xylene	2.0061	13.67	14.20	0.82
	o-Xylene	2.0061	13.44	10.42	0.84
2	*p*-Xylene	2.0062	13.53	7.78	
	m-Xylene	2.0062	13.55	7.70	
	o-Xylene	2.0062	13.53	7.50	

Temperature Dependence of β-H HFCC. The signal pattern in Fig. 6 as well as in Fig. 7 was found to

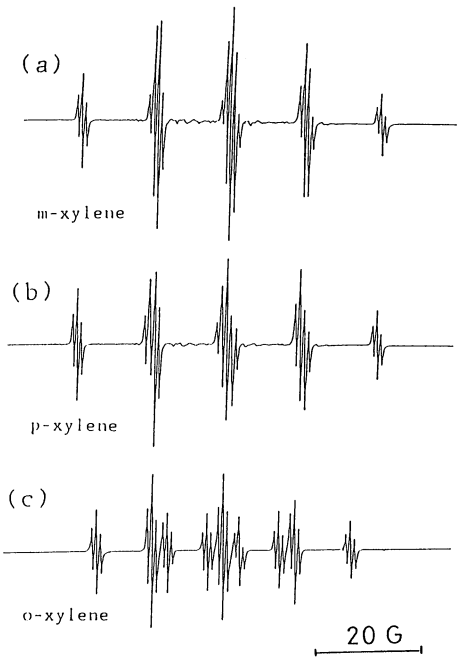

Fig. 6. ESR spectrum appeared during the thermal decomposition of DBPO in the presence of **1** in (a) *m*-xylene, (b) *p*-xylene, and (c) *o*-xylene.

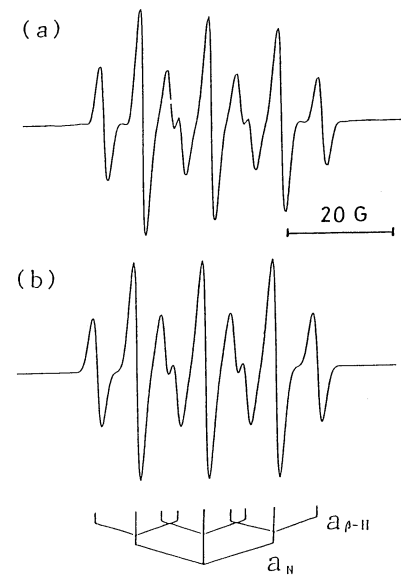

Fig. 7. (a) ESR spectrum obtained during the thermal decomposition of DBPO in the presence of **2** in *m*-xylene. (b) Simulation spectrum.

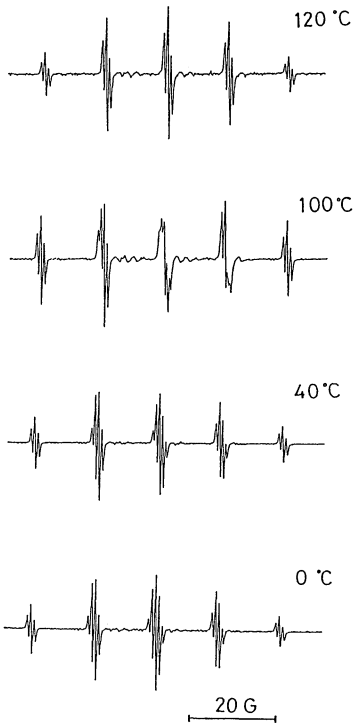

Fig. 8. Temperature dependence of ESR spectrum of the adduct formed during the DBPO decomposition in the presence of **1** in *m*-xylene.

change with temperature. A representative one is shown in Fig. 8. It was found by inspection of these signals that the hfcc of the two (equivalent) β-hydrogens varies with temperature, while no substantial line broadening with temperature occurs. It follows therefore, that the rotation around the N–CH_2 bond is severely restricted. The β-H hfcc values at various temperatures are given in Table 3. In Fig. 9, the β-H hfcc is plotted against temperature for the **1-BZ** adducts. It is seen that the temperature coefficient is negative for each adduct, but is very small for the *o*-methylbenzyl adduct. In contrast to this, the temperature coefficients are all positive for the **2-BZ** adducts (Table 3).

There are a vast of theoretical and experimental investigations which relate the hfcc of β-hydrogens to their conformational positions. A review by Sullivan and Mengen[22] may be instructive. According to Stone and Maki,[23] hindered internal rotations give rise to a temperature-dependent β-H hfcc. For adducts such as ours, it is too difficult to take into account vicinal group effects properly in estimating the torsional barrier. However, it can qualitatively be said that the steeper the torsional barrier becomes, the smaller the temperature coefficient is, as observed for *o*-substituted adducts.

On the basis of theoretical background, our adducts will have either A or B conformation according to the steric situations.

Table 3. Variation of the β-H HFCC with Temperature

Solvent	Temperature/°C	Trap 1 $a_{\beta\text{-H}}$/G	Trap 2 $a_{\beta\text{-H}}$/G
p-Xylene	100	14.05	
	80	14.20	
	60	14.35	7.90
	40	14.55	7.78
	20	14.78	7.64
	0	14.98	7.53
	−20	15.28	7.36
	−40	15.40	7.36
m-Xylene	100	13.68	
	80	13.87	7.92
	60	14.00	7.84
	40	14.20	7.70
	20	14.45	7.56
	0	14.65	7.36
	−20	14.93	7.25
	−40	15.23	7.06
	−60	15.43	6.94
	−80		6.72
o-Xylene	100	10.28	
	80		7.78
	60	10.36	7.62
	40		7.50
	20	10.49	7.36
	0		7.22
	−20	10.55	7.03
	−40		6.89
	−60		6.69
	−80		6.24

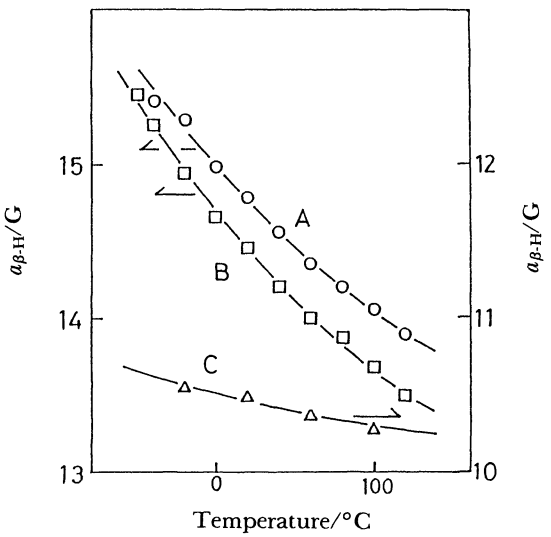

Fig. 9. Plots of β-H hfcc against temperature for **1-BZ** adducts in (A) *p*-xylene, (B) *m*-xylene, and (C) *o*-xylene.

It has been accepted that the hfs of the β-hydrogens is caused by the hyperconjugation interaction of the p-π orbital on N atom with a pseudo π-molecular orbital

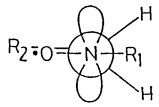

A

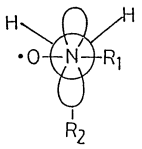

B

of the type $\phi=\chi_{s1}-\chi_{s2}$ where χ_{s1} and χ_{s2} denote the s-orbitals of the two β-hydrogens. In conformation A, the two orbitals are in preferable positions to each other, resulting in a large β-H hfcc (Table 3). As temperature increases, a fluctuation from the optimum position will take place, and this gives rise to a negative temperature coefficient of β-H hfcc. In conformation B, the temperature coefficient will be positive by just the opposite reason. It follows that the conformation of the **1-BZ** adducts is A and that of **2-BZ** adducts is B. For the o-methylbenzyl adduct, the steric hindrance will become the greatest among the similar adducts. A very small temperature coefficient and remarkably reduced β-H hfcc for this adduct is in harmony with the above statement.

References

1) N. Nishimura, K. Takeda, and Y. Furumatsu, *Aust. J. Chem.*, **42**, 823 (1989).

2) S. Terabe and R. Konaka, *J. Chem. Soc., Perkin 2*, **1973**, 369.

3) S. Terabe, K. Kuruma, and R. Konaka, *J. Chem. Soc., Perkin 2*, **1973**, 1252.

4) P. D. Bartlett, E. P. Benzing, and R. E. Pincock, *J. Am. Chem. Soc.*, **82**, 1762 (1960), and references therein.

5) P. J. Krusic, P. Meakin, and J. P. Tesson, *J. Phys. Chem.*, **75**, 3438 (1971).

6) K. S. Chen, P. J. Krusic, P. Meakin, and J. K. Kochi, *J. Phys. Chem.*, **78**, 2014 (1974).

7) P. D. Sullivan and E. M. Menger, *Adv. Magn. Reson.* **9**, 9 (1977).

8) E. H. Bartlett, C. Eaborn, and D. R. M. Walton, *J. Chem. Soc. C*, **1970**, 1434.

9) Y. Ogata and S. Sawaki, *Tetrahedron*, **23**, 3327 (1967).

10) L. I. Smith and F. L. Taylor, *J. Am. Chem. Soc.*, **57**, 2370 and 2460 (1935).

11) R. Okazaki and N. Inamoto, *J. Chem. Soc. B*, **1970**, 1586.

12) N. A. Milas and D. M. Surgenor, *J. Am. Chem. Soc.*, **68**, 205 (1946).

13) M. Shiotani, S. Murabayashi, and J. Sohma, *Int. J. Radia. Phys. Chem.*, **8**, 483 (1976).

14) I. I. Bilkis and S. M. Shein, *Tetrahedron*, **31**, 969 (1975).

15) A. Mackor, Th. A. J. W. Wajer, Th. J. de Boer, and J. D. W. van Voorst, *Tetrahedron Lett.*, **1967**, 385.

16) C. Chatgilialoglu, V. Malatesta, and K. U. Ingold, *J. Phys. Chem.*, **84**, 3597 (1980).

17) C. Chatgilialoglu and K. U. Ingold, *Can. J. Chem.*, **59**, 1745 (1981).

18) C. Chatgilialoglu and K. U. Ingold, *J. Phys. Chem.*, **86**, 4372 (1982).

19) Landolt-Börnstein, "New Series; Band II, 9c, 1," Springer-Verlag, Berlin (1977).

20) A. L. Williams, E. A. Oberright, and J. W. Brooks, *J. Am. Chem. Soc.*, **78**, 1190 (1956).

21) T. Nishikawa and K. Someno, *Bull. Chem. Soc. Jpn.*, **47**, 2881 (1974).

22) P. D. Sullivan and E. M. Menger, "Advances in Magnetic Resonance," ed by J. S. Waugh, Academic Press, New York (1977), Vol. 9, pp. 1—48.

23) E. W. Stone and A. H. Maki, *J. Chem. Phys.*, **37**, 1326 (1962).